

See discussions, stats, and author profiles for this publication at: <http://www.researchgate.net/publication/282252456>

Pathways and Hydrography in the Mesoamerican Barrier Reef System Part 1: Circulation

ARTICLE *in* CONTINENTAL SHELF RESEARCH · OCTOBER 2015

Impact Factor: 1.89 · DOI: 10.1016/j.csr.2015.09.014

READS

19

5 AUTHORS, INCLUDING:



Laura Carrillo

El Colegio de la Frontera Sur

18 PUBLICATIONS 144 CITATIONS

SEE PROFILE



John T. Lamkin

National Oceanic and Atmospheric Adminis...

40 PUBLICATIONS 157 CITATIONS

SEE PROFILE



John Largier

University of California, Davis

162 PUBLICATIONS 4,029 CITATIONS

SEE PROFILE



Pathways and Hydrography in the Mesoamerican Barrier Reef System Part 1: Circulation



L. Carrillo ^{a,*}, E.M. Johns ^b, R.H. Smith ^b, J.T. Lamkin ^c, J.L. Largier ^d

^a El Colegio de la Frontera Sur, Departamento de Sistemática y Ecología Acuática, Av. Centenario km 5.5, Col. Pacto Obrero, 77014 Chetumal, Quintana Roo, Mexico

^b NOAA Atlantic Oceanographic and Meteorological Laboratory, 4301 Rickenbacker Causeway, Miami, FL 33149, USA

^c NOAA National Marine Fisheries Service, Southeast Fisheries Science Center, 75 Virginia Beach Drive, Miami, FL 33149, USA

^d Bodega Marine Laboratory, University of California Davis, PO Box 247, Bodega Bay, CA 94923, USA

ARTICLE INFO

Article history:

Received 13 May 2015

Received in revised form

23 August 2015

Accepted 12 September 2015

Available online 21 September 2015

Keywords:

Yucatan Current

Mesoamerican Reef

Circulation

Mesoscale

Gyres

ABSTRACT

Acoustic Doppler Current Profiler (ADCP) measurements and surface drifters released from two oceanographic cruises conducted during March 2006 and January/February 2007 are used to investigate the circulation off the Mesoamerican Barrier Reef System (MBRS). We show that the MBRS circulation can be divided into two distinct regimes, a northern region dominated by the strong, northward-flowing Yucatan Current, and a southern region with weaker southward coastal currents and the presence of the Honduras Gyre. The latitude of impingement of the Cayman Current onto the coastline varies with time, and creates a third region, which acts as a boundary between the northern and southern circulation regimes. This circulation pattern yields two zones in terms of dispersal, with planktonic propagules in the northern region being rapidly exported to the north, whereas plankton in the southern and impingement regions may be retained locally or regionally. The latitude of the impingement region shifts interannually and intra-annually up to 3° in latitude. Sub-mesoscale features are observed in association with topography, e.g., flow bifurcation around Cozumel Island, flow wake north of Chinchorro Bank and separation of flow from the coast just north of Bahía de la Ascension. This third feature is evident as cyclonic recirculation in coastal waters, which we call the Ascension-Cozumel Coastal Eddy. An understanding of the implications of these different circulation regimes on water mass distributions, population connectivity, and the fate of land-based pollutants in the MBRS is critically important to better inform science-based resource management and conservation plans for the MBRS coral reefs.

© 2015 Elsevier Ltd. All rights reserved.

1. Introduction

The Mesoamerican Barrier Reef System (MBRS) lies in the western Caribbean, in coastal waters off Mexico, Belize, Guatemala and Honduras (Fig. 1a). It is the second largest coral reef system in the world, and the largest coral reef system in the Atlantic Ocean. The MBRS is receiving increased attention in international marine resource conservation plans, due to its biodiversity and also its connectivity with other ecosystems located in the Gulf of Mexico, Cuba, and the Straits of Florida.

Most of the MBRS is characterized by a narrow continental shelf (< 10 km) and the reef area is aligned with the coast. Off-shore, reef habitat is found around Cozumel Island and four major atolls: Chinchorro Bank, Turneffe Reef, Lighthouse Reef and Glovers Reef (Fig. 1). The shelf is wider in the area of the Bay Islands

off the Honduras coast and along the northernmost coast of the Yucatan Peninsula (near Contoy Island). Further east there are two deep basins (Cayman Basin and Yucatan Basin), which are separated by a ridge extending from southeastern Cuba to Belize (Fig. 1). The MBRS is located in the northwestern corner of the Caribbean circulation system (Fig. 1a), as the flow adjusts to the Yucatan Peninsula and enters the Gulf of Mexico through the Yucatan Channel.

The Caribbean Sea surface circulation is comprised of westward flow with speeds of 0.5–1.0 m/s (Kinder, 1983; Schmitz and McCartney, 1993; Gallegos and Czitrom, 1997; Mooers and Maul, 1998; Andrade and Barton, 2000; Johns et al., 2002), which transports ~28 Sv from the Atlantic Ocean. This inflow is divided in approximately equal thirds between the Windward Islands passages south of Martinique (~10 Sv), the Leeward Islands (~8 Sv), and the Greater Antilles passages between Puerto Rico and Cuba (~10 Sv) (Johns et al., 2002). The largest individual contributions occur through Grenada Passage (~6 Sv) and Windward Passage (~7 Sv) (Johns et al., 2002). This flow forms the

* Corresponding author.

E-mail addresses: lcarrillo@ecosur.mx, laucarrillo@gmail.com (L. Carrillo).

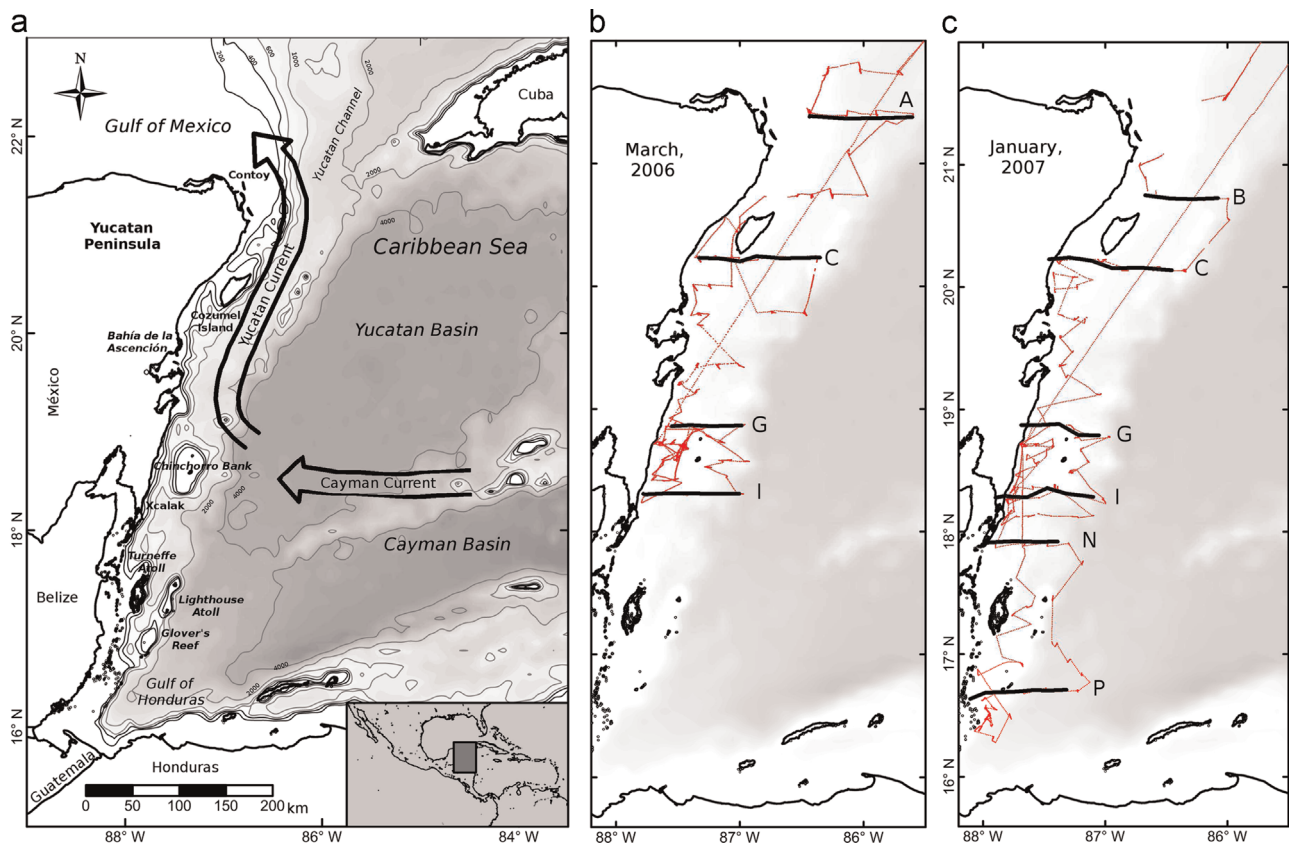


Fig. 1. (a) Study area showing basins and other selected bathymetric features of the Mesoamerican Barrier Reef System (MBRS). Bathymetry is shaded in gray, with contours at 1000, 2000, 3000, and 4000 m, as well as at 200, 400 and 600 m along the narrow shelf. (b) March 2006 survey track. (c) January 2007 survey track.

Caribbean Current with numerous large and energetic eddies associated with the large-scale flow (Molinari et al., 1981; Carton and Chao, 1999; Murphy et al., 1999; Andrade and Barton, 2000; Pratt and Maul, 2000; Oey et al., 2004; Centurioni and Niiler, 2003; Richardson, 2005). Using altimetry, numerical models, and Lagrangian drifters, it has been shown that these gyres and mesoscale eddies usually travel from east to west at speeds of approximately 0.15 m/s (Carton and Chao, 1999), and some may enter the Gulf of Mexico through the Yucatan Channel. These meanders and loops are the major source of kinetic energy variability in the Caribbean circulation system (Pratt and Maul, 2000; Alvera-Azcárate et al., 2009).

When the Caribbean Current passes through the Cayman Basin it becomes the Cayman Current, flowing westward along $19 \pm 2^\circ\text{N}$ (Badan et al., 2005), before turning northward along the Yucatan Peninsula to form the Yucatan Current (Badan et al., 2005; Cetina et al., 2006). The Yucatan Current is a strong and persistent warm current with speeds up to 2 m/s, which enters the Gulf of Mexico as a jet (Ochoa et al., 2001; Sheinbaum et al., 2002; Oey et al., 2004) and develops into the Loop Current. Ultimately this flow exits the Gulf of Mexico through the Straits of Florida, forming the Florida Current and eventually the Gulf Stream in the western North Atlantic Ocean (Mooers and Maul, 1998; Gallegos and Czirom, 1997).

The coastal circulation in the MBRS has been primarily studied using numerical models (Murphy et al., 1999; Barnier et al., 2001; Johns et al., 2002; Sheng and Tang, 2004; Ezer et al., 2005; Cherubin et al., 2008). Most observations are concentrated in the Yucatan Channel (Candela et al., 2002; Ochoa et al., 2001; Candela et al., 2003; Oey et al., 2004; Rousset and Beal, 2010, 2011). The few observations from farther south in the MBRS include mooring data in the Mexican Caribbean (Cetina et al., 2006) and Cozumel

Channel (Chávez et al., 2003; Ochoa et al., 2005). While most numerical models of the region resolve mesoscale features with grid sizes of $\sim 5\text{--}50\text{ km}$ (Oey and Lee, 2003; Sheng and Tang, 2004; Ezer et al., 2005), a few very-high-resolution models ($\sim 50\text{ m}$ grid) have resolved small-scale circulation patterns near Belizean coral reefs and their impact on the dispersion of eggs and larvae (Ezer et al., 2011, 2012). A spatially extensive description of the circulation along the MBRS has not been developed previously.

As part of a large-scale program of larval and hydrographic surveys designed to provide a fisheries oceanography baseline for the Western Caribbean during the winter spawning season, oceanographic cruises were conducted during March 2006 and January/February 2007. The primary motivation for studying the MBRS circulation is to provide a better description and understanding of currents and water mass distributions that could affect biological connectivity within and between ecosystems. During these oceanographic cruises, hydrographic and current data were collected in conjunction with larval fish samples derived from net tows. In addition, satellite-tracked surface drifters were deployed to track the surface circulation and elucidate transport pathways.

The aim of this manuscript is to provide, for the first time, a description of the coastal circulation off the MBRS. We present this description of the regional circulation with an eye for features important for the distribution of living resources in the MBRS. We hope to provide scientific information that can be used by resource managers. Herein, we present the first part of the Pathways and Hydrography in the MBRS study (Part 1), focused on the regional circulation of the MBRS, and we provide background for a companion paper on the hydrographic characteristics of the MBRS (henceforth referred to as Part 2).

2. Data and methods

Oceanographic cruises in March 2006 (March 18–April 1, 2006) and January (January 14–30, 2007) 2007 (hereafter M06 and J07) aboard the NOAA Ship *Gordon Gunter* surveyed the MBRS (Fig. 1b and c). The station array was selected to provide a measure of larval fish diversity and abundance while also resolving the major oceanographic features, involving a trade-off between density of stations and spatial coverage. During M06, the Mexican Caribbean was surveyed from the Yucatan Channel south to the border of Belize while most of the MBRS was covered in J07, south to the Gulf of Honduras off Belize.

Current velocity measurements were obtained from a hull-mounted Acoustic Doppler Current Profiler (ADCP: RD Instruments 75 kHz Ocean Surveyor, model OS75). These shipboard ADCP data were post-processed using standard Common Ocean Data Access System (CODAS) tools and processing software from the University of Hawaii (http://currents.soest.hawaii.edu/docs/doc/codas_doc/adcp_processing.html). The ADCP data were reduced to five-minute averages and vertical bin sizes of 10 m. No data are available close to the ADCP and the shallowest data are for a bin that extends from 30 to 40 m depth (nominally 35 m). Transects oriented perpendicular to the coastline (Fig. 1b and c) are used to describe the continuity and evolution of the current structure: Line A, the northernmost transect from the shelf off Contoy Island; Line C, a transect off Tulum passing just south of Cozumel Island; Line G, a transect across the northern edge of Chinchorro Bank; Line I, a transect just south of Chinchorro Bank; Line N, a transect off the Belizean coast near the mouth of Chetumal Bay; and Line P, the southernmost transect, just south of

Glovers Reef and representative of Belizean coastal waters in the Gulf of Honduras. Lines N and P were only occupied during 2007.

Further, to characterize regional surface transport pathways, seventeen ARGOS satellite-tracked surface drifters were deployed. These drifters were provided by NOAA's Global Drifter Program (<http://www.aoml.noaa.gov/phod/dac/index.php>). They consist of a surface buoy and a subsurface drogue centered at 15 m.

3. Results

3.1. Near-surface circulation from shipboard ADCP

Fig. 2a and b shows the ADCP-observed circulation off the MBRS at 35 m depth during M06 and J07. The circulation at depth shows a similar pattern with lower speeds, as described in the next section. The primary feature is the Yucatan Current, flowing from south to north along the boundary of the northern Yucatan Peninsula.

During the M06 survey, the Yucatan Current is well-defined north of Chinchorro Bank ($\sim 19^\circ\text{N}$) all the way to the Yucatan Channel ($\sim 22^\circ\text{N}$), with a clear acceleration from the south ($\sim 0.52\text{ m/s}$) to the north (up to $\sim 2.35\text{ m/s}$). Around Chinchorro Bank the flow is more complex. The westward flow east of the bank diverges to pass the atoll along both the northern and southern coasts, but both arms of the flow turn to the north to form the Yucatan Current. Further to the north, near Cozumel Island, the Yucatan Current bifurcates, with one part flowing through the Cozumel Channel between mainland Mexico and Cozumel Island, and the other part flowing east of Cozumel Island.

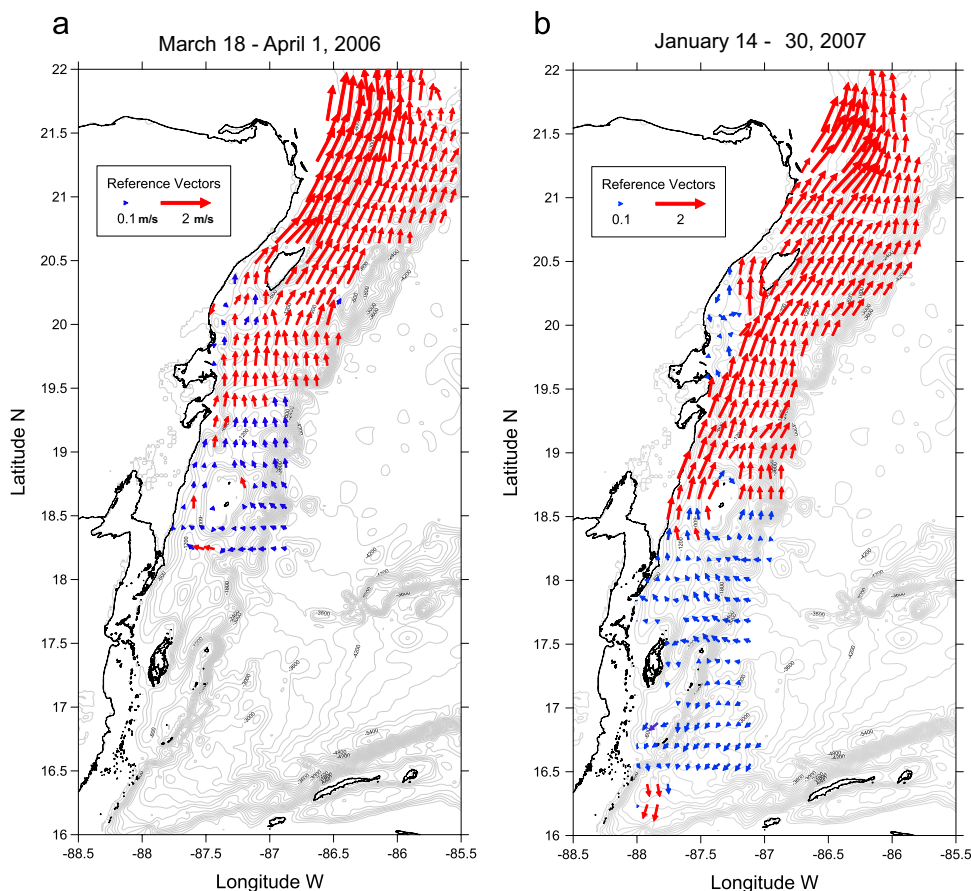


Fig. 2. Velocity vectors showing the horizontal surface circulation from shipboard ADCP measurements at 35 m: (a) March 2006 and (b) January 2007. Speeds lower than 0.5 m/s are colored in blue, and speeds higher than 0.5 m/s are colored in red. (For interpretation of the references to color in this figure legend, the reader is referred to the web version of this article.)

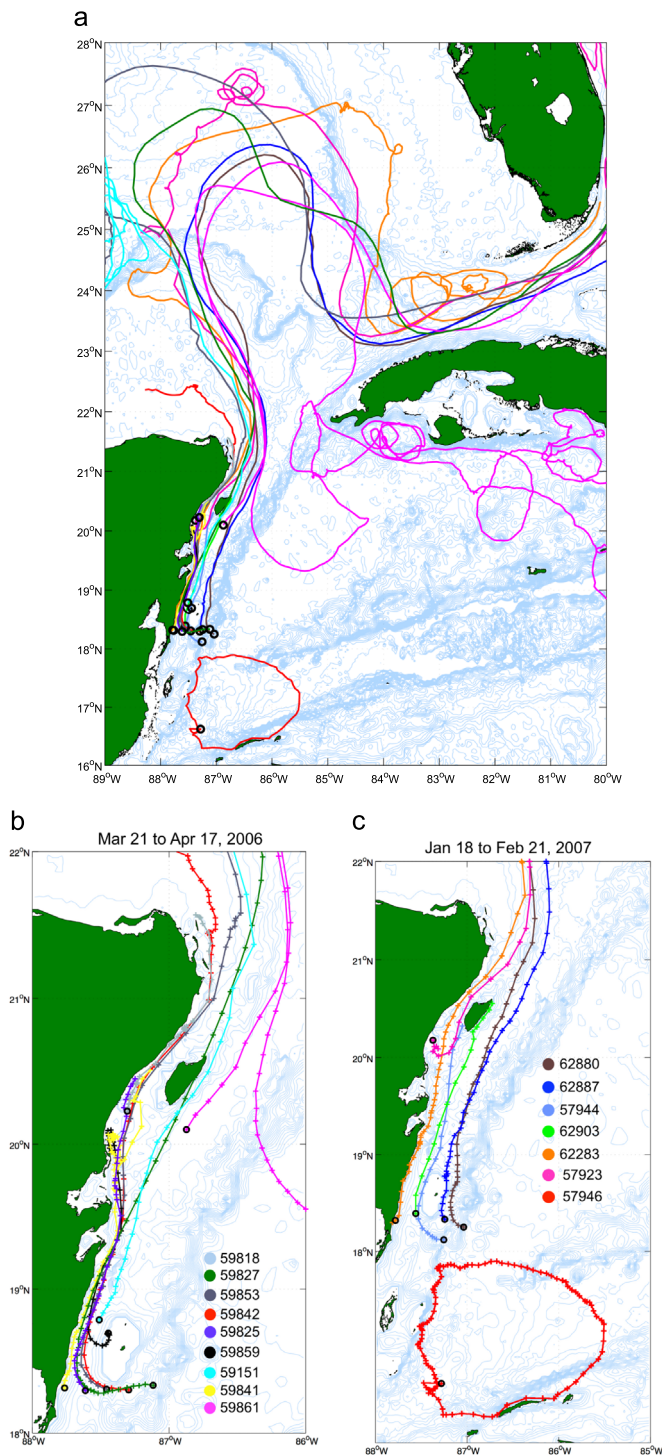


Fig. 3. (a) Trajectories of all drifters deployed during March 2006 and January 2007, showing connectivity between the MBRS, the Gulf of Mexico, waters off south Florida, and waters off Cuba. One drifter returned to the Caribbean. All drifters were drogued at 15 m depth. (b) Trajectories from drifters released during March 2006 along the MBRS: each point represents a 6-h subsampled location of a drifter. (c) Trajectories from drifters released during January 2007 on the MBRS: each point represents a 6-h subsampled location of a drifter. The Gulf of Honduras Gyre was delineated by the trajectory of one of the released drifters.

North of Cozumel Island, the current intensifies attaining speeds > 2 m/s in the Yucatan Channel. Inshore between Cozumel Island and Bahía de la Ascension, slow and reversed flows are observed, forming a cyclonic recirculation with speeds up to 0.5 m/s.

During the J07 survey, the Yucatan Current is well-defined

already south of Chinchorro Bank ($\sim 18.3^\circ\text{N}$) and the current is fairly uniform in speed (~ 1.10 m/s) until it approaches the Yucatan Channel. As in 2006, the Yucatan Current bifurcates around Cozumel Island, and around Chinchorro Bank. Also, the flow separation along the mainland north of Bahía de la Ascension is again evident and extending further offshore (~ 30 km). From south of Chinchorro Bank down to the Gulf of Honduras, the velocity field is an order of magnitude weaker than observed farther north in the Yucatan Current. The surface circulation off the Belizean coast shows a weak onshore flow that diverges around latitude 17.25°N (near the Turneffe Reef and Lighthouse Reef atolls), with waters north of this latitude moving into the Yucatan Current and waters south of this latitude entering the Gulf of Honduras. The observed divergence around 17°N confirms the pattern, which previously has been suggested by numerical model simulations (Sheng and Tang, 2004; Ezer et al., 2005).

3.2. Surface circulation from satellite-tracked drifters

Drifter trajectories during the M06 and J07 cruises are shown in Fig. 3a–c. The drifters were deployed at 17 sites off the MBRS. These drifter trajectories are used to delineate transport pathways and to illustrate the connectivity between the MBRS and ecosystems in the Gulf of Mexico, as well as in western Cuba, and south Florida (Fig. 3a, Table 1).

During M06, nine drifters were released. Five drifters were released south of Chinchorro Bank (Fig. 3b: $\sim 18.3^\circ\text{N}$, ID numbers 59825, 59827, 59842, 59841 and 59853). These drifters started to move westward until they were near the coast, at which point they turned northward and joined a coast-parallel current. Three of the drifters continued northward in the Yucatan Current (one east of Cozumel Island) and were exported into the Gulf of Mexico and seemed trapped by the Loop Current. The other two drifters (ID numbers 59841 and 59825) remained closer to the coast north of $\sim 19.5^\circ\text{N}$ and slowed down or reversed direction in the coastal waters off Bahía Ascension before running aground at $\sim 20.4^\circ\text{N}$ and $\sim 20.5^\circ\text{N}$ (drifter ID number 59841 being retained off Bahía Ascension for a few days). A sixth drifter (ID number 59859), deployed on the western edge of Chinchorro Bank, was retained there moving slowly southward before being entrained into the northward flow closer to the mainland. This drifter was also closer to the shore around $\sim 19.5^\circ\text{N}$ and entrained into a recirculation feature just north of Bahía Ascension for a few days before grounding $\sim 20.0^\circ\text{N}$. The seventh drifter (ID number 59151) deployed NW of Chinchorro Bank was quickly entrained into the northward flow, joining the Yucatan Current flowing east of Cozumel Island and into the Gulf of Mexico. The eighth drifter (ID number 59818) was deployed at the southern entrance of the Cozumel Channel, close to the shore, so that it moved southward at first, before being entrained into the northward flow through the channel; however, it remained close to the coast and finally grounded near Contoy Island $\sim 21.5^\circ\text{N}$, where the Yucatan Current separates from the Yucatan Peninsula. One of the Chinchorro drifters was also detrained from the current near Contoy, stalling for a couple of days (ID 59842; Fig. 3b), but it did not run aground and was re-entrained into the Yucatan Current. The final drifter (ID 59861) was released offshore, southeast of Cozumel Island. It moved quickly northward, exiting the Caribbean – but it returned to the Caribbean months later on the eastern side of the Yucatan Channel and spent several months in the eddy field just south of Cuba (Fig. 3a). This drifter trajectory illustrates the direct connectivity between the MBRS and the ecosystems located in the Gulf of Mexico and along the southern coast of Cuba.

During J07, seven drifters were released (Fig. 3c). Again five were deployed south of Chinchorro – one near the mainland village of Xcalak (ID numbers 62880, 62887, 57944, 62903 and

Table 1
Summary of satellite tracked drifters released during March 2006 and January 2007 cruises. Information includes drifter ID numbers, release dates, deployment positions, and fate.

Drifter ID	Initial date	Deployment position		Fate
		Latitude N	Longitude W	
59151	28/03/2006	–87.511	18.787	Left the Caribbean
59818	21/03/2006	–87.306	20.227	Grounded North of Yucatan
59825	01/04/2006	–87.612	18.296	Grounded Riviera Maya
59827	01/04/2006	–87.116	18.333	Left the Caribbean
59841	02/04/2006	–87.764	18.314	Grounded Riviera Maya
59842	01/04/2006	–87.295	18.3	Left the Caribbean
59853	01/04/2006	–87.457	18.305	Left the Caribbean
59859	28/03/2006	–87.444	18.694	Grounded North of Bahia Asencion
59861	03/04/2006	–86.873	20.1	Left and re-enter the Caribbean
62283	23/01/2007	–87.782	18.32	Left the Caribbean
62880	23/01/2007	–87.037	18.251	Left the Caribbean
62887	23/01/2007	–87.244	18.331	Left the Caribbean
62903	23/01/2007	–87.56	18.392	Grounded Cozumel Island
57944	31/01/2007	–87.254	18.119	Grounded Cozumel Island
57946	26/01/2007	–87.281	16.623	Gulf of Honduras
57923	18/01/2007	–87.372	20.177	Left the Caribbean

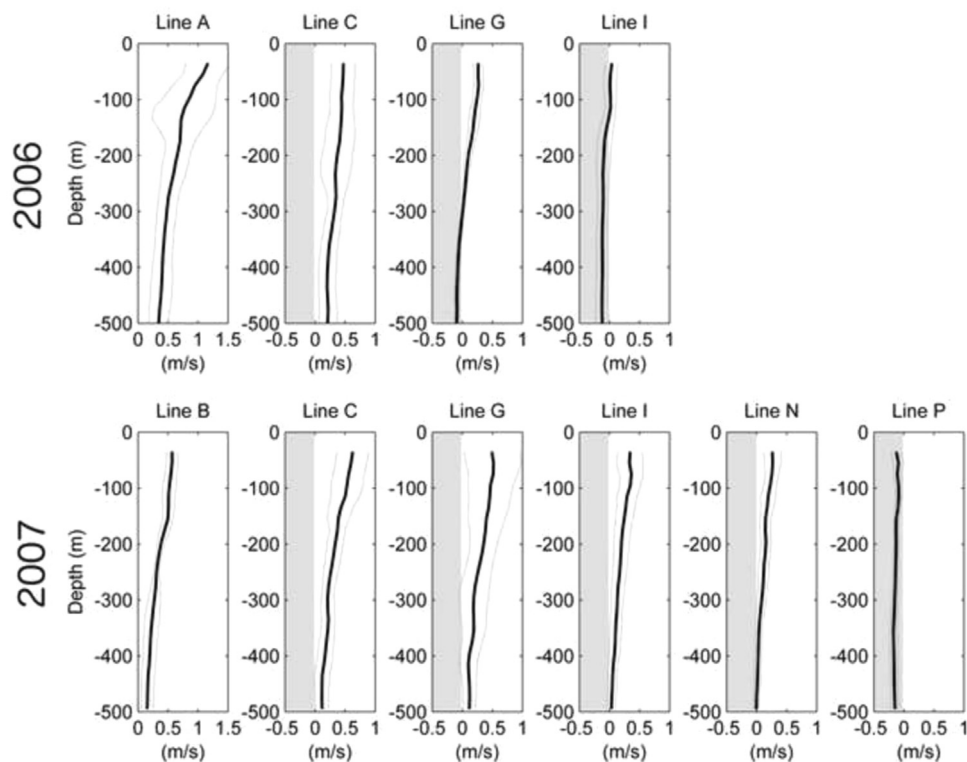


Fig. 4. Average northward velocity profiles for selected transects. Dark solid lines show the mean value, dashed lines show the standard deviation, and the gray shaded area shows negative velocity values (southward velocity). Panels in the top row represent transects in March 2006, and panels in the bottom row represent transects in January 2007.

62283). The offshore drifters moved onshore and then turned to the north, with all five drifters being entrained into the Yucatan Current, although the nearshore one moved slowly between 19.0°N and 19.5°N while the drifter in the core of the current reached Cozumel in only four days (at a speed of ~ 0.64 m/s). A sixth drifter (ID number 57923) was released north of Bahía Asencion, in the separation zone where it moved slowly southward before being entrained into the northward current. The seventh drifter (ID number 57956) deployed near the Gulf of Honduras ($\sim 16.5^{\circ}\text{N}$) slowly described a loop that delineates a mesoscale cyclonic gyre (the Honduras Gyre) about 200 km in diameter. This loop was completed in 25 days, at a speed of 0.25–

0.31 m/s. After moving back onshore at $\sim 17.8^{\circ}\text{N}$ it moved south along the wall of the reef area, past Lighthouse Reef and Glovers Reef atolls, before running aground at a similar latitude to where it was released. While the Honduras Gyre has been seen in numerical models (Sheng and Tang, 2004; Ezer et al., 2005), there are very few direct observations.

3.3. Vertical structure of the velocity field

Mean velocity profiles to 500 m depth were obtained along cross-shore transects for both M06 and J07 (Fig. 4). With the exception of Line P in the south ($\sim 16^{\circ}\text{N}$), northward flow is observed

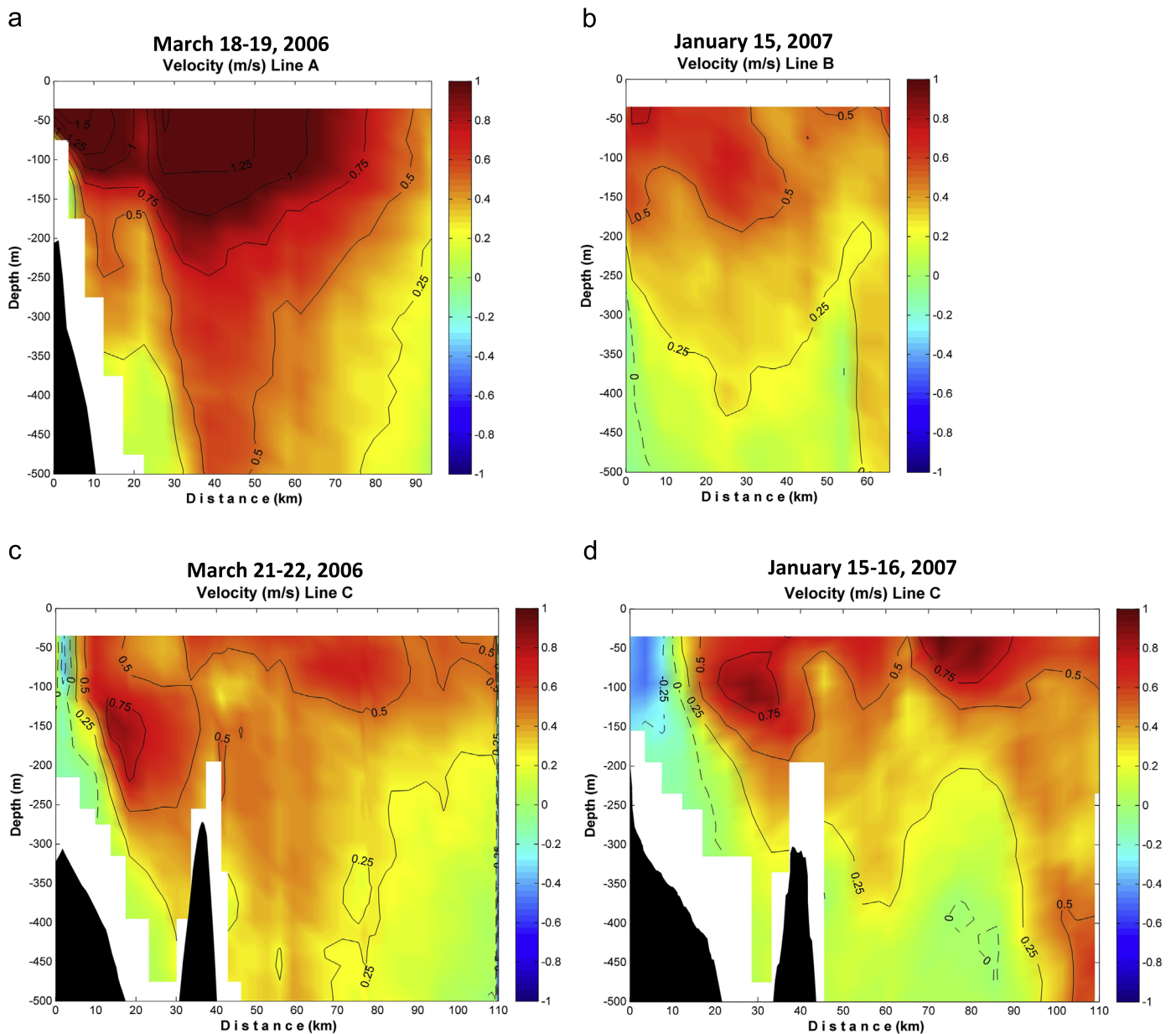


Fig. 5. Vertical structure of velocity fields from shipboard ADCP for the northern MBRS transects: (a) Yucatan Channel, Line A, March 2006; (b) Northern Cozumel Island, Line B, January 2007; (c) Southern Cozumel Island, Line C, March 2006; and (d) Southern Cozumel Island, Line C, January 2007.

near-surface on all transects. Although weakening with depth, this northward flow extends to at least 500 m in the northern region, which is dominated by the well-organized Yucatan Current – Lines A and C in M06 when the Yucatan Current starts $\sim 19.0^\circ\text{N}$ (Section 3.1); Lines B, C, G and I in J07 (Section 3.1). On transects in the impingement region (Lines G and I in M06; Line N in J07) the northward flow is weaker at the surface and reverses at depth. On Line P in the southern region, flow is uniformly weak and southward at all depths. The velocity magnitude decreased from north to south by about an order of magnitude.

The vertical and cross-shore structure of flow on these transects is shown in Figs. 5–7. On the northernmost line in the Yucatan Channel (Line A) the Yucatan Current was 100 km wide with the strongest magnitudes found in the surface and subsurface layers (above 200 m), but extending throughout the entire 500 m of the water column in mid-channel (Fig. 5a). As no data are available from Line A in J07, data are shown for Line B (Fig. 5b). Here the Yucatan Current was weaker (~ 0.75 m/s) and with the core located

in the uppermost 75 m (and possibly inshore of the transect).

On Line C, immediately upstream of Cozumel Island, a more complex pattern of northward flow was observed (Fig. 5c and d). In both years the branch west of the Island is well-defined, with a core centered between 100–150 m depth and speeds up to ~ 0.9 m/s. On the eastern side of Cozumel Island the northward flow showed speeds with a maximum of 0.7 m/s during M06 and up to 1.0 m/s during J07. In contrast to northward flow offshore, a zone of southward flow is observed close to the coast in both years – flow speeds up to 0.37 m/s extending ~ 10 km from the coast during M06, and 0.5 m/s extending more than 20 km from the coast in J07.

On lines G and I, north and south of Chinchorro Bank, there were marked differences between M06 and J07 (Fig. 6), consistent with the latitudinal shift in the impingement region. During M06, the Yucatan Current formed north of Chinchorro Bank, so flows across these transects were weak (~ 0.2 m/s or weaker); stronger flow was seen only offshore on the transect north of Chinchorro Bank (Line G, Fig. 6a). On Line I, this weak northward flow reversed

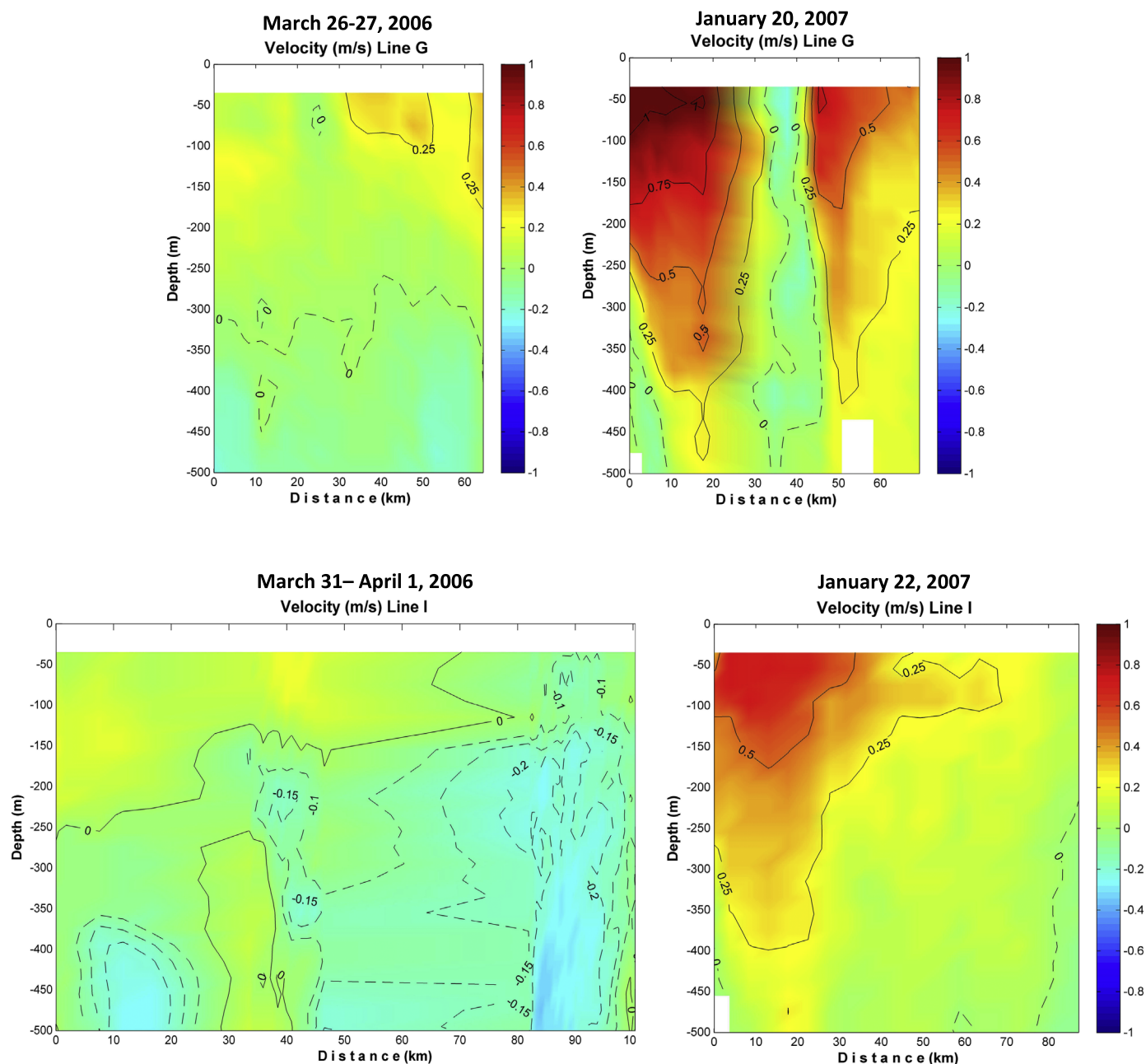


Fig. 6. Vertical structure of velocity fields from shipboard ADCP for transects past Chinchorro Bank: (a) Northern Chinchorro, Line G, March 2006; (b) Northern Chinchorro Line G January 2007; (c) Southern Chinchorro Line I March 2006; and (d) Southern Chinchorro Line I January 2007.

offshore and at depth (Fig. 6c), with weak southward flow at depth. During J07, the Yucatan Current formed south of Chinchorro Bank so that northward flow was observed on both transects (Fig. 6b and d). The strongest flow was observed in the channel between the mainland and the Bank, exceeding 1 m/s at the surface near the coast on Line G (Fig. 6b). Immediately downstream of Chinchorro Bank (Line G), a wake region was observed with weak and reversed flow at all depths, strongest at the surface (~ 0.2 m/s). Southward flow was also observed at depth offshore on the Line I, comparable with that at depth offshore on Line G in M06. Some northward flow was observed near-surface even on Line N ($\sim 18.0^\circ\text{N}$), but it was weaker and shallower than on Lines I and G (Fig. 7a). On the southernmost transect of the MBRS, Line P, flow is weakly southward and uniform in depth (Fig. 7b and also Fig. 4).

4. Discussion

We have used shipboard ADCP data and satellite-tracked surface drifters from two oceanographic cruises conducted in March 2006 and January–February 2007 to investigate the circulation off the MBRS. Coherent spatial structures are evident throughout the region and circulation can no longer be simply characterized by the well-recognized Yucatan Current that flows northward into the Gulf of Mexico. These new observations show that while the Yucatan Current is dominant in the northern MBRS, the circulation in the southern region is weaker and more complex where flow patterns may reverse as part of the cyclonic circulation known as the Honduras Gyre. There is also a transition region or impingement region in the central MBRS. In J07, the Yucatan Current was well defined south of Chinchorro Bank ($\sim 18.3^\circ\text{N}$), whereas in M06 it formed only north of Chinchorro Bank ($\sim 19.0^\circ\text{N}$). In M06 a

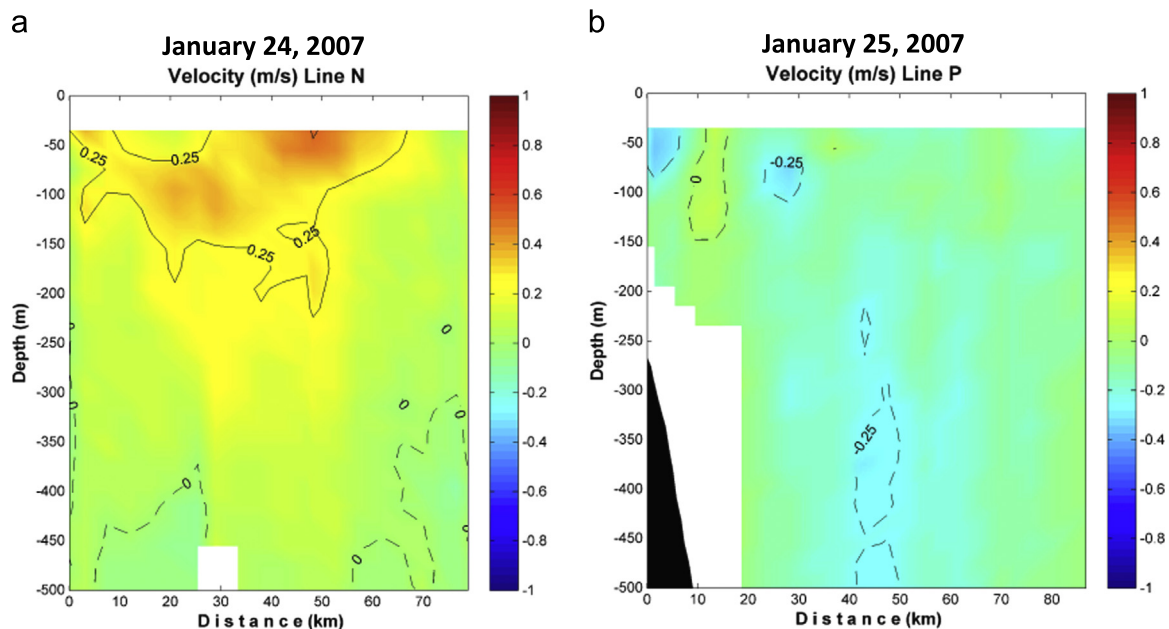


Fig. 7. Vertical structure of velocity fields from shipboard ADCP for transects off the southern MBRS: (a) Belizean coast, transect N, January 2007; and (b) Gulf of Honduras, Line P, January 2007.

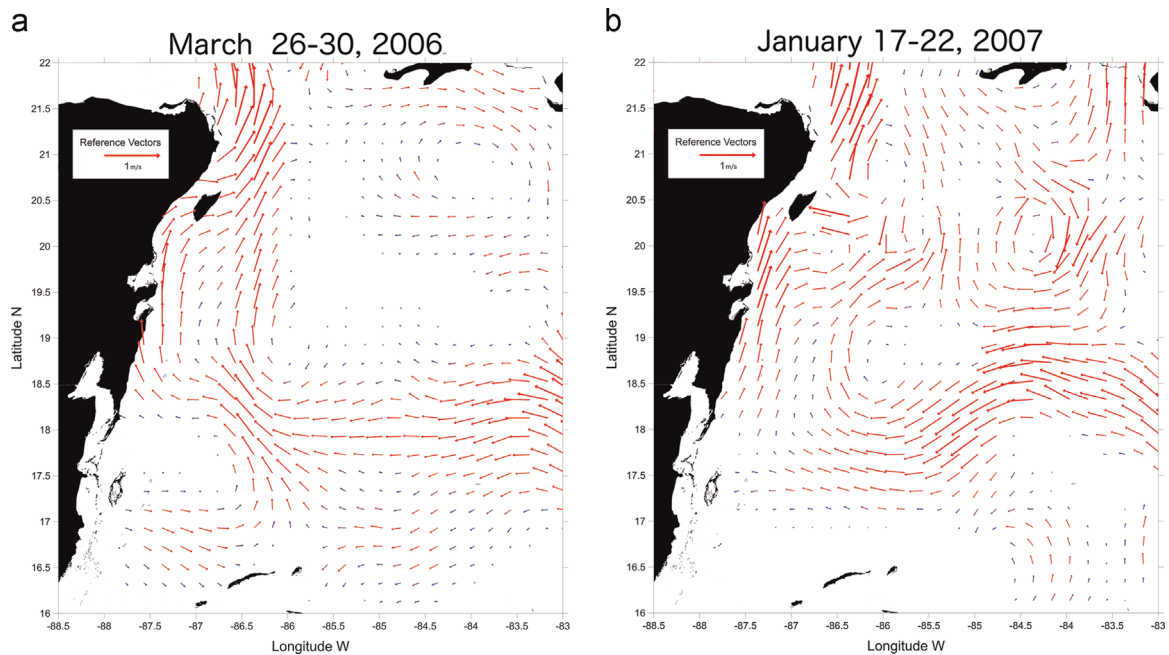


Fig. 8. Geostrophic velocity fields derived from altimetry from the Rio05 output model (Rio and Hernandez 2004). The fields correspond to a 10-day period up to the cruise dates; (a) For March 2006; and (b) For January 2007. Speeds lower than 0.2 m/s are colored in blue, and speeds higher than 0.2 m/s are colored in red. (For interpretation of the references to color in this figure legend, the reader is referred to the web version of this article.)

westward flow impinges on the Bank and a divergence was observed along the eastern side, with flow passing north and south of Chinchorro Bank, before reorganizing and turning northward to form the Yucatan Current (Fig. 2). In contrast, in J07 flow approaches the Bank from the south, and a strong northward current is observed between the Bank and the mainland. Weaker northward flow was observed as far south as 17.5°N, with coherent southward flow observed only south of 17.0°N.

It is not possible to generalize seasonal and interannual variability in the mesoscale circulation of the MBRS with these two surveys. Nevertheless, our observations show temporal variability in the MBRS circulation and specifically in the impingement

location of the Cayman Current. The difference between the two observed winter flow fields may be due to the mesoscale variability associated with the meandering of the Cayman Current and the propagation of eddies, as suggested by numerical models and altimeter data (Ezer et al., 2005, 2012) or due to latitudinal migration of the Cayman Current. Through analysis of altimeter data, Alvera-Azcárate et al. (2009) show that variability in the Caribbean circulation is strongest at the annual time scale, followed by higher frequency variability due in part to eddy propagation through the Caribbean. There are 4.6 eddies per year according to estimates by Pratt and Maul, (2000). Interannual variability is also important (spectral peak around 4 years), contributing about a quarter of the

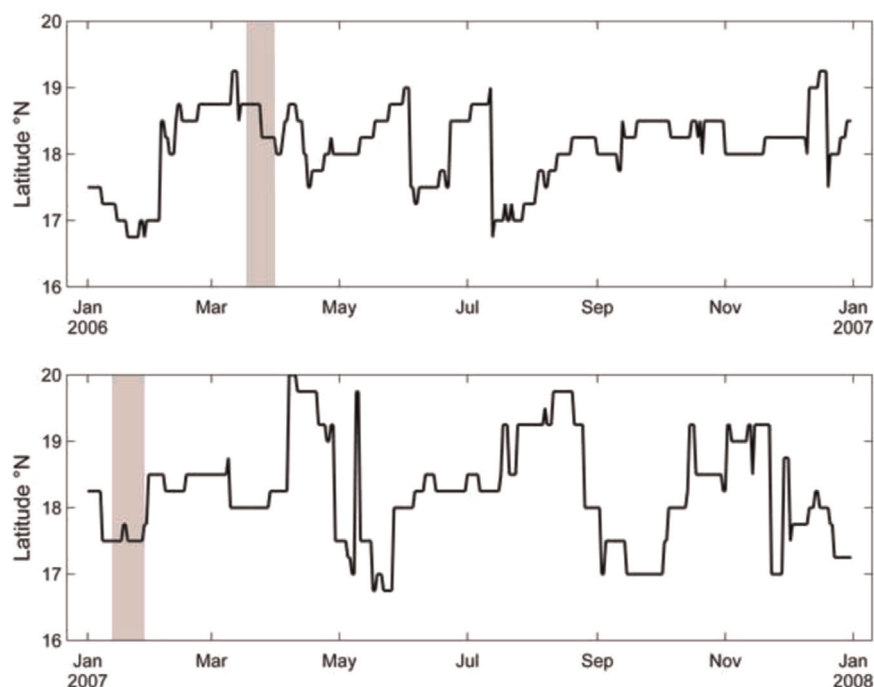


Fig. 9. Time series of the latitude of the core of the Cayman Current, determined from the maximum value of the zonal component of the geostrophic currents derived from altimetry. (a) 2006; and (b) 2007. Gray shadowed areas represent the time period of the cruises.

annual variance (Alvera-Azcárate et al., 2009). More observations throughout the year are needed to separate the effects of eddies, seasonal cycle and interannual variations – as also suggested by numerical modeling (Ezar et al., 2005, 2012).

Arising from these new observations are three new insights, discussed below: (i) the role of the impinging Cayman Current in defining coastal circulation along the MBRS; (ii) the presence of several sub-mesoscale features associated with flow-topography interactions, and (iii) the implications of this circulation structure and variability on the dispersal of larvae and other planktonic organisms.

4.1. Impingement of the Cayman Current on the coast

When the Cayman Current impinges upon the Yucatan Peninsula, most of its water flows northward into the Yucatan Current, while a small portion flows southward into the Honduras Gyre (Badan et al., 2005). Here we show that between the northern region, characterized by strong northward flow (Yucatan Current), and the southern region, characterized by weak southward flow (Honduras Gyre), is a transitional or impingement region that spans about 1° latitude – but this impingement zone shifts north and south by a few degrees latitude with shifts in the zonal axis of the Cayman Current. As spatial coverage of our shipboard ADCP data does not extend far offshore, we use sea-surface-height data from satellite altimetry. Geostrophic currents from the Rio05 output model are estimated from dynamic topography averaged over a 10-day period (Rio and Hernandez 2004) and used here because they resolve spatial scales of order 10 km (Rio and Hernandez 2004). The mean velocity fields from altimetry data during our surveys show impingement on the MBRS and formation of the Yucatan coastal boundary current further north in M06 and further south in J07 (Fig. 8a and b). During M06, the core of the Cayman Current impinges at ~ 18.3 – 18.8°N (i.e., near Chinchorro Bank; Fig. 8a), whereas during J07 it impinges farther south at ~ 17.5 – 17.7°N (i.e., in Belizean waters, Fig. 8b). The Yucatan Current can be observed in both years, accelerating through the

Yucatan Channel (Fig. 8a and b). These observations, obtained from satellite altimetry, agree well with ADCP-measured velocity fields.

To further explore latitudinal variability in the core of the Cayman Current, we look for the maximum east–west speed in a spatial domain bounded by 16 – 20°N latitude and 84 – 88°W longitude. The latitude of the core of the current, calculated from altimetry data, shifts between 16.5°N and 20.0°N over the 2-year period of 2006 and 2007 (Fig. 9a and b). This is consistent with prior results that show that the Cayman Current flows along $19 \pm 2^\circ\text{N}$ (Badan et al., 2005; Sheng and Tang, 2004; Ezer et al., 2005). Our observations combined with altimeter data show that the Cayman Current impinged on the Yucatan coast around Chinchorro Bank ($\sim 18.75^\circ\text{N}$) during M06 and further south in Belizean waters ($\sim 17.5^\circ\text{N}$) during J07 (Figs. 8a and b and 9a and b). Although the latitude of impingement of the Cayman Current shifted less than 1° between the M06 and J07 cruises, marked differences in flow patterns were observed off the MBRS – specifically in the Chinchorro region. Wherever the Cayman Current impingement occurs, a transitional zone develops between the strong and well-defined Yucatan Current regime in the northern portion of the MBRS and the weaker current regime in the southern portion of the MBRS. In the less energetic southern region, mesoscale eddies may play an important role, e.g., the cyclonic eddy at 17.5°N and 87°W in M06 (Fig. 8a). Based on numerical modeling, Ezar et al. (2005, 2011) suggest that mesoscale eddies may be responsible for reversal of offshore flows in Belizean waters (south of the impingement zone). Anticyclonic flow structures further north and offshore (e.g., at 19°N 86°W in M06 and J07 – Fig. 8a and b) are less likely to dominate coastal circulation along the MBRS. However, more observations are needed to identify and evaluate the effect of mesoscale eddies along the MBRS and in the meandering of the Cayman Current. Alternatively, how strong is the seasonal variability in the impingement of Cayman Current? A long-term observational program is needed to investigate further seasonal and interannual variability as well as the eddy climatology and effects in the waters off the MBRS.

4.2. Sub-mesoscale flow features

While impingement of the Cayman Current and northward flow of the Yucatan Current along the coastal boundary dominate the regional circulation, several small-scale features emerge from these observations, including flow separation in the vicinity of Bahía de la Ascension and near Contoy Island and wake effects downstream of Cozumel Island and Chinchorro Bank.

Most notable is the identification of a cyclonic recirculation feature in coastal waters around 20°N, inshore of the northward flow that separates from the coastal boundary around 19.5°N, at the southern headland defining Bahía de la Ascension (Figs. 2a and b and 3b), and where isobaths show marked curvature. This sub-mesoscale feature extends north of Line C (Fig. 5c and d) into the Cozumel Channel, thus spanning about 1° latitude (~100 km) alongshore, but extending only 10–20 km from the coast. In addition to ADCP data, four drifters retained in this small-scale feature for a few days or more help demarcate the extent of the feature and drifters not entrained into the recirculation demarcate the separation line that bounds the feature on the east. The presence of this feature during both cruises, and during days following the cruises when drifters were retained, indicates that it is a persistent feature, which we call the Ascension-Cozumel Coastal Eddy. It is comparable to features elsewhere, such as the “upwelling shadow” regions along the Californian coast (Graham and Largier, 1997), where flow separates from headlands. Most directly comparable is the Durban Eddy found in the Natal Bight (South Africa), where the Agulhas Current separates briefly from the coast (Schumann, 1988; Lutjeharms, 2006), yielding cyclonic flow and plankton retention evident in enhanced chlorophyll levels.

A second feature of note is the wake evident downstream of Chinchorro Bank, both during westward flow past the Bank in M06 and during northward flow past the Bank in J07. In M06 a drifter released on the western flank on the Bank moves south (anticyclonically) slowly and is only entrained into the coastal current a few days later (Fig. 3b). In J07 the ADCP transect north of the Bank shows a marked southward flow in the wake (Fig. 6b) and a drifter released south of the Bank stalls for a couple of days at the northeast corner of the Bank, presumably entrained in the bank's wake.

4.3. Dispersal distances in the MBRS

The marked difference in flow patterns between the northern, southern and impingement regions of the MBRS will lead to important differences in the transport of plankton and pollutants in this ecosystem. To investigate/illustrate differences in dispersal outcome along the MBRS, progressive-vector displacements were calculated from velocity time series derived from altimetry data. At each of six locations off the MBRS coast (Fig. 10), velocity was integrated over a week to obtain a potential displacement (implicitly assuming uniform flow). These week-long displacements were calculated for each site and for each week over the 2-year period of interest (2006–2007). This “progressive-vector” analysis provides no information on actual fate of a planktonic particle, but rather is used as a measure of transport tendency at this location, expressed in a dispersal-relevant way (e.g., Roughan et al. 2005). North–south displacements are labeled Y, and east–west displacements are labeled X. While a quasi-Gaussian distribution in the displacement is observed for most sites, there are marked differences in north–south bias.

The northernmost part of the MBRS (site 1, Fig. 10) is characterized by persistent northward transport and rapid export of plankton from the Caribbean to the Gulf of Mexico via the Yucatan Current. Displacements exceeded 100 km and often attained 400 km or more. At site 2, alongshore displacements were shorter

than at site 1, with the mode being less than 100 km – this reduction in speed probably due to the blocking effect of Cozumel Island located just to the north. At site 3, again displacements are invariably to the north, with a mode of ~250 km.

In contrast to the dominant northward transport in the northern region, in the southern region displacements are shorter and switch between northward and southward, with a mode close to zero in near-coastal waters (sites 5 and 6) – a flow scenario that can lead to retention of a small subset of plankton (Largier, 2003). Further offshore at site 5, stronger northward displacements are observed.

These results are based on a coarse velocity field calculated from altimeter data (Rio05 data with 10 km resolution) and do not resolve small-scale features that can be important for dispersal of coastal species (Ezer et al., 2011, 2012). However, the large-scale contrast between transport in the northern and southern regions is dramatic and consistent with the results of Muhling et al. (2013), using historical surface drifter trajectories in the same geographical area. Muhling et al. (2013) also used net tow data collected during the M06 and J07 cruises to show that there was a marked difference in larval fish variety, abundance, and distribution between the northern and southern parts of the MBRS.

5. Conclusion

The circulation in the MBRS during winter cruises in 2006 and 2007 can be characterized by three regions: a northern region with a well-defined Yucatan Current, a southern region with weak southward flow, and a transitional region where the Cayman Current impinges upon the Yucatan Peninsula. There is a marked gradient in velocity from north to south, with northward velocity through the Yucatan Channel more than an order of magnitude stronger than velocities further south. In the northern region where the Yucatan Current dominates the circulation, some small-scale features were observed where flow separation occurred, for example forming a wake downstream of Chinchorro Bank and the Ascension-Cozumel Coastal Eddy downstream of Bahía de la Ascension. At larger scales, the most important time-dependent factor appears to be the latitude at which the Cayman Current impinges on the coast, with the impingement region shifting 3° latitude north and south over the years. The Yucatan Current only forms to the north of this impingement region, around 19°N in M06 and around 18.3°N in J07 – north and south of Chinchorro Bank, respectively.

In addition to more data on the persistence of these patterns, there is a critical need for interdisciplinary studies that link these circulation patterns to the dispersion of plankton and pollutants in this MBRS region. The Cayman/Yucatan Current system has important biological implications, with a tendency for retention and the possibility of local recruitment in the southern and impingement regions, while northward advection and connectivity with the Gulf of Mexico are expected in the northern region. There are a number of known spawning areas and reproductive sites along the MBRS coast, most of which have been documented in the southern MBRS (Aguilar-Perrera and Aguilar-Dávila, 1996; Heyman et al., 2008; Sosa-Cordero et al., 2009). Important questions include whether there is a quantifiable relationship between spawning sites and dispersal/retention characteristics associated with coastal circulation patterns, and whether local retention zones are a critical factor for population persistence for species in this region. Smaller scale flow patterns are also important, with tidal currents and flow-topography interactions having significant influence on the initial dispersion of eggs/larvae immediately after spawning (Heyman et al., 2005; Heyman et al., 2008; Ezer et al., 2011; Hamner and Largier, 2012). More observational studies off

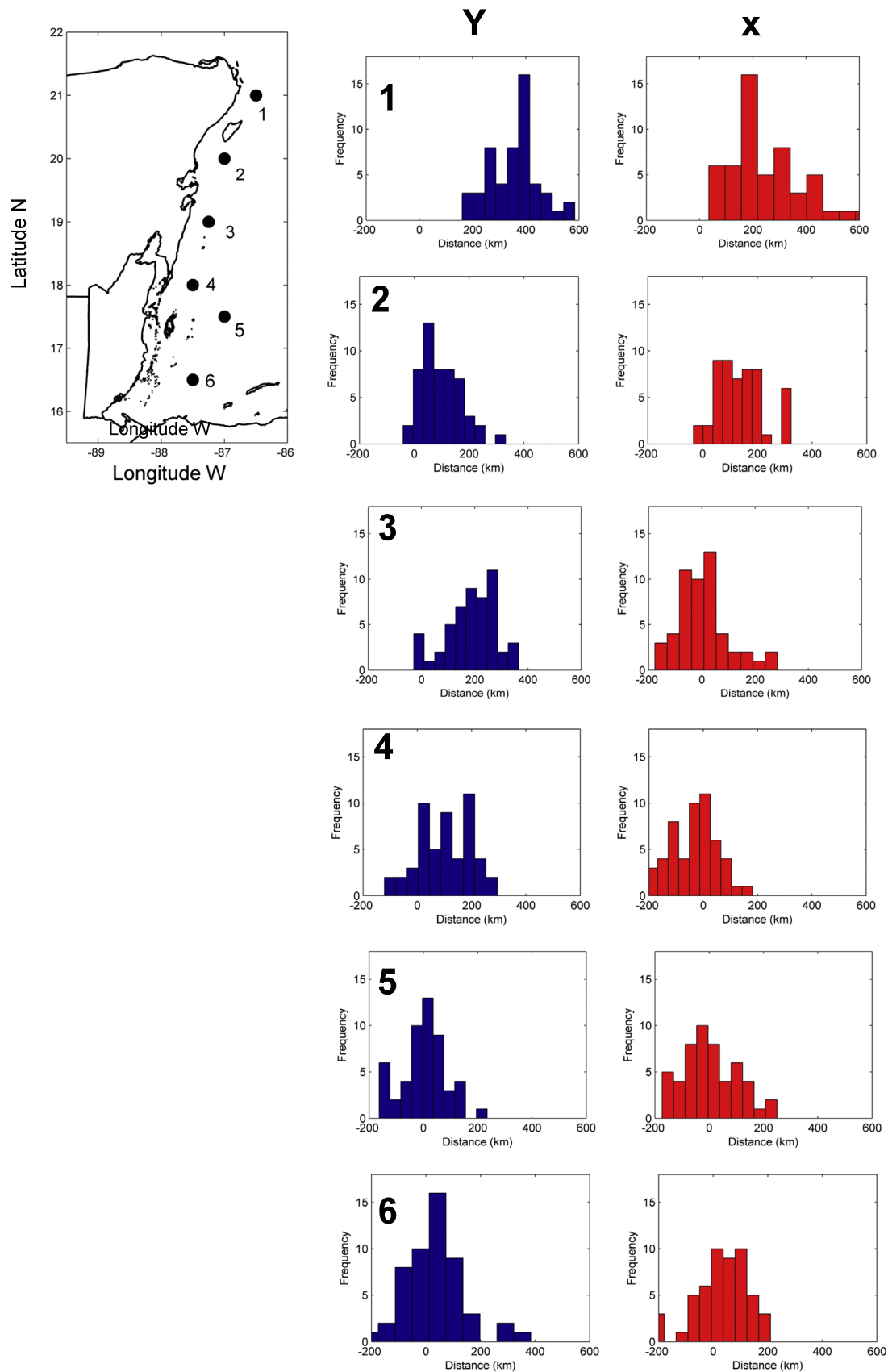


Fig. 10. “Progressive-vector” displacement calculated from velocities derived from altimetry data at six locations along the MBRS. Displacements are calculated by integrating current over one week. Y values represent the meridional direction, with positive values representing northward displacement. X displays represent the zonal direction, with positive values representing eastward displacement.

the MBRS are needed to understand the role of local and oceanic forcing in the dispersal of eggs and larvae.

Based on these new observations, the circulation off the MBRS can no longer be simply described as part of the overall broader Caribbean circulation system, but rather as a variable and dynamic region with complexity over a wide range of spatial and temporal scales. Our results provide new insights as well as data to allow the validation of large-scale model simulations of circulation off the MBRS. In order to inform science-based resource management and marine conservation in this reef area, we need to improve our understanding of the influence of regional circulation variability on the connectivity of ecosystems and the fate of land-based pollutants in the MBRS over different seasons and years. For this, it is critically important to establish long-term, sustained interdisciplinary observations of the oceanography and ecology of MBRS coral reef ecosystems.

Acknowledgments

ADCP data were provided to NOAA Coral Reef Conservation Program and are on file at the Southeast Fisheries Science Center (SEFSC) Library. ARGOS satellite-tracked surface drifter data can be found at NOAA's Global Drifter Program (<http://www.aoml.noaa.gov/phod/dac/index.php>). This work was partially supported by the base funding of NOAA's Atlantic Oceanographic and Meteorological Laboratory and Southeast Fisheries Science Center. Partial support for L. Carrillo was provided by ECOSUR. Ship time was provided by NOAA under the projects Larval Fish and Physical Oceanography Survey of the Mesoamerican Reef System, and Meso-American System Transport and Ecology Research. We thank the Captain and crew of the NOAA Ship *Gordon Gunter*.

References

- Aguilar-Perrera, A., Aguilar-Dávila, W., 1996. A spawning aggregation of Nassau grouper, *Ephinephelus striatus* (Pisces: Serranidae), in the Mexican Caribbean. *Environ. Biol. Fishes* 45, 351–361.
- Alvera-Azcárate, A., Barth, A., Weisberg, R.H., 2009. The surface circulation of the Caribbean Sea and the Gulf of Mexico as inferred from satellite altimetry. *J. Phys. Oceanogr.* 39 (3), 640–657. <http://dx.doi.org/10.1175/2008JP03765.1>.
- Andrade, C.A., Barton, E.D., 2000. Eddy development and motion in the Caribbean Sea. *J. Geophys. Res.* 105 (C11), 26191–26201.
- Badan, A., Candela, J., Sheinbaum, J., Ochoa, J., 2005. Upper-layer circulation in the approaches to Yucatan Channel. Circulation in the Gulf of Mexico: Observations and Models (Geophysical Monograph series), AGU, vol. 161, pp. 57–69.
- Barnier, B., Reynaud, T., Beckmann, A., Böning, C., Jolines, J.M., Barnard, S., Jia, Y., 2001. On the seasonal variability and eddies in the North Brazil Current: insights from model intercomparison experiments. *Prog. Oceanogr.* 48 (2–3), 195–230. [http://dx.doi.org/10.1016/S0079-6611\(01\)00005-2](http://dx.doi.org/10.1016/S0079-6611(01)00005-2).
- Candela, J., Tanahara, S., Crepon, M., Barnier, B., Sheinbaum, J., 2003. Yucatan Channel flow: observations versus CLIPPER ATL6 and MERCATOR PAM models. *J. Geophys. Res.* 108 (C12), 1–24. <http://dx.doi.org/10.1029/2003JC001961>.
- Candela, J., Sheinbaum, J., Badan, A., Leben, R., 2002. The potential vorticity flux through the Yucatan Channel and the Loop Current in the Gulf of Mexico. *Geophys. Res. Lett.* 29 (22), 2–5. <http://dx.doi.org/10.1029/2002GL015587>.
- Carton, J., Chao, Y., 1999. Caribbean Sea eddies inferred from TOPEX/Poseidon altimetry and a 1/6° Atlantic Ocean model simulation. *J. Geophys. Res.* 104 (C4), 7743–7752. <http://dx.doi.org/10.1029/1998JC900081>.
- Centurioni, L.R., Niiler, P., 2003. On the surface currents of the Caribbean Sea. *Geophys. Res. Lett.* 30 (6), 10–13. <http://dx.doi.org/10.1029/2002GL016231>.
- Cetina, P., Candela, J., Sheinbaum, J., Ochoa, J., Badan, A., 2006. Circulation along the Mexican Caribbean coast. *J. Geophys. Res.* 111 (C8), 1–19. <http://dx.doi.org/10.1029/2005JC003056>.
- Chávez, G., Candela, J., Ochoa, J., 2003. Subinertial flows and transports in Cozumel Channel. *J. Geophys. Res.* 108 (C2), 1–11. <http://dx.doi.org/10.1029/2002JC001456>.
- Cherubin, L.M., Kuchinke, C.P., Park, C.B., 2008. Ocean circulation and terrestrial runoff dynamics in the Mesoamerican region from spectral optimization of SeaWiFS data and a high resolution simulation. *Coral Reefs* 27, 503–551. <http://dx.doi.org/10.1007/s00338-007-0348-1>.
- Ezer, T., Thattai, D.V., Kjerfve, B., Heyman, W.D., 2005. On the variability of the flow along the Meso-American Barrier Reef system: a numerical model study of the influence of the Caribbean current and eddies. *Ocean Dyn.* 55, 458–475. <http://dx.doi.org/10.1007/s10236-005-0033-2>.
- Ezer, T., Heyman, W.D., Houser, C., Kjerfve, B., 2011. Modeling and observations of high-frequency flow variability and internal waves at a Caribbean reef spawning aggregation site. *Ocean Dyn.* 61, 581–598. <http://dx.doi.org/10.1007/s10236-010-0367-2>.
- Ezer, T., Heyman, W.D., Houser, C., Kjerfve, B., 2012. Extreme flows and unusual water levels near a Caribbean coral reef: was this a case of a “perfect storm”? *Ocean Dyn.* 62, 1045–1057. <http://dx.doi.org/10.1007/s10236-012-0545-5>.
- Gallegos, A., Czitrom, S., 1997. Aspectos de la oceanografía física regional del Mar Caribe. In: Lavín, M.F. (Ed.), *Oceanografía Física en México*, Monografía 3. Unión Geofísica Mexicana, México, D.F., pp. 1401–1414.
- Graham, W.M., Largier, J.L., 1997. Upwelling shadows as nearshore retention sites: the example of northern Monterey Bay. *Cont. Shelf Res.* 17 (5), 509–532.
- Hamner, W.M., Largier, J.L., 2012. Oceanography of the planktonic stages of aggregation spawning reef fishes. Chapter 6 in *Reef Fish Spawning Aggregations: Biology, Research and Management*, Fish & Fisheries Series 35, Springer, pp. 159–190. doi: 10.1007/978-94-007-1980-4_6.
- Heyman, W.D., Kjerfve, B., Graham, R.T., Rhodes, K.L., Garbutt, L., 2005. Spawning aggregations of *Lutjanus cyanopterus* (Cuvier) on the Belize Barrier Reef over a 6 year period. *J. Fish Biol.* 67, 83–101.
- Heyman, W., Kjerfve, B., Ezer, T., 2008. Mesoamerican reef spawning aggregations help maintain fish population: a review of connectivity research and priorities for science and management. In: Grober-Dunsmore, R., Keller, B.D. (Eds.), *Caribbean Connectivity: Implications for Marine Protected Area Management*. Silver Spring, MD, pp. 150–169, Marine Sanctuaries Conservation Series ONMS-08-07, NOAA.
- Johns, W.E., Townsend, T.L., Fratantoni, D.M., Wilson, W.D., 2002. On the Atlantic inflow to the Caribbean Sea. *Deep Sea Res. Part I: Oceanogr. Res. Pap.* 49 (2), 211–243. [http://dx.doi.org/10.1016/S0967-0637\(01\)00041-3](http://dx.doi.org/10.1016/S0967-0637(01)00041-3).
- Kinder, T.H., 1983. Shallow currents in the Caribbean Sea and Gulf of México as observed with satellite-tracked drifters. *Bull. Mar. Sci.* 33 (2), 239–246.
- Largier, J.L., 2003. Considerations in estimating larval dispersal distances from oceanographic data. *Ecol. Appl.* 13 (1), S71–S89, Supplement.
- Lutjeharms, J.R.E., 2006. *The Agulhas Current*. Springer-Verlag, Berlin.
- Mooers, C., Maul, G.A., 1998. Intra-Americas Sea coastal ocean circulation. In: Robinson, K.H., Brink, K.H. (Eds.), *The Sea* vol. 11. John Wiley & Sons, New York, pp. 183–208.
- Molinari, R., Spillane, M., Brooks, I., Atwood, D., Duckett, C., 1981. Surface currents in the Caribbean Sea as deduced from Lagrangian observations. *J. Geophys. Res.* 86 (C7), 6537–6542.
- Muhling, B.A., Smith, R.H., Vasquez-Yeomans, L., Lamkin, J.T., Johns, E.M., Carrillo, L., Sosa-Cordero, E., Malca, E., 2013. Larval reef fish assemblages and mesoscale oceanographic structure along the Mesoamerican Barrier Reef System. *Fish. Oceanogr.* 22 (5), 409–428. <http://dx.doi.org/10.1111/fog.12031>.
- Murphy, S.J., Hurlburt, H.E., O'Brien, J., 1999. The connectivity of eddy variability in the Caribbean Sea, the Gulf of Mexico, and the Atlantic Ocean. *J. Geophys. Res.* 104 (C1), 1431–1453.
- Ochoa, J., Candela, J., Badan, A., Sheinbaum, J., 2005. Ageostrophic fluctuations in Cozumel Channel. *J. Geophys. Res.* 110, 1–16. <http://dx.doi.org/10.1029/2004JC002408>.
- Ochoa, J., Sheinbaum, J., Badan, A., Candela, J., Wilson, D., 2001. Geostrophy via potential vorticity inversion in the Yucatan Channel. *J. Mar. Res.* 59 (5), 725–747. <http://dx.doi.org/10.1357/002224001762674917>.
- Oey, L.Y., Lee, H.C., 2003. Effects of winds and Caribbean eddies on the frequency of Loop Current eddy shedding: a numerical model study. *J. Geophys. Res.* 108 (C10), 1–25.
- Oey, L.-Y., Ezer, T., Sturges, W., 2004. Modeled and observed empirical orthogonal functions of currents in the Yucatan Channel. *J. Geophys. Res.* 109, C08011. <http://dx.doi.org/10.1029/2004JC002345>.
- Pratt, R.W., Maul, G.A., 2000. Sea surface height variability of the Intra-Americas Sea from Topex/Poseidon satellite altimetry: 1992–1995. *Bull. Mar. Sci.* 67 (2), 687–708.
- Richardson, P., 2005. Caribbean Current and eddies as observed by surface drifters. *Deep Sea Res. Part II: Top. Stud. Oceanogr.* 52 (3–4), 429–463. <http://dx.doi.org/10.1016/j.dsr2.2004.11.001>.
- Rio, M.H., Hernandez, F., 2004. A mean dynamic topography computed over the world ocean from altimetry, in situ measurements, and a geoid model. *J. Geophys. Res.* 109, C12032. <http://dx.doi.org/10.1029/2003JC002226>.
- Rousset, C., Beal, L.M., 2010. Observations of the Florida and Yucatan Currents from a Caribbean cruise ship. *J. Phys. Oceanogr.* 40 (7), 1575–1581. <http://dx.doi.org/10.1175/2010JP044471>.
- Rousset, C., Beal, L.M., 2011. On the seasonal variability of the currents in the Straits of Florida and Yucatan Channel. *J. Geophys. Res.* 116 (C8), 1–17. <http://dx.doi.org/10.1029/2010JC006679>.
- Roughan, M., Mace, A.J., Largier, J.L., Morgan, S.G., Fisher, J.L., Carter, M.L., 2005. Subsurface recirculation and larval retention in the lee of a small headland: a variation on the upwelling shadow theme. *J. Geophys. Res.* 110, C10027. <http://dx.doi.org/10.1029/2005JC002898>.
- Schmitz, W.J., McCartney, M.S., 1993. On the North Atlantic circulation. *Rev. Geophys.* 31 (1), 29–49.

- Sheinbaum, J., Candela, J., Badan, A., Ochoa, J., 2002. Flow structure and transport in the Yucatan Channel. *Geophys. Res. Lett.* 29 (3), 1–4. <http://dx.doi.org/10.1029/2001GL013990>.
- Sheng, J., Tang, L., 2004. A two-way nested-grid ocean circulation model for the Meso-American Barrier Reef system. *Ocean Dyn.* 54 (2), 232–242. <http://dx.doi.org/10.1007/s10236-003-0074-3>.
- Schumann, E.H., 1988. Physical oceanography off natal. In: Schumann, E.H. (Ed.), *Lecture Notes on Coastal and Estuarine Studies*. Springer-Verlag, New York, pp. 101–130.
- Sosa-Cordero, E., Ramírez-González, A., Olivares-Escobedo, J., 2009. Programa de ordenamiento pesquero del Estado de Quintana Roo. 1. Pesquería de meros y especies afines. Informe Final CONAPESCA-SAGARPA. Chetumal, Quintana Roo, México: El Colegio de la Frontera Sur, p. 110.